Electronic Supplementary Information

Exploring the oxygen electrode bi-functional activity of Ni-N-C doped graphene system with N, C co-ordinations and OH ligand effects

Zhao Liang,[a,†] Mingming Luo,[a,†] Mingwei Chen,[a,†] Xiaopeng Qi,[a] Juan Liu,[b] Chao Liu,[a,c,*] Shaik Gouse Peera,[d,*] Tongxiang Liang[a,*]

[a] Engineering Research Center for Hydrogen Energy Materials and Devices, Faculty of Materials Metallurgy and Chemistry, Jiangxi University of Science and Technology, Ganzhou 341000, China

[b] Department of Mining and Materials Engineering, McGill University, Montreal, QC H3A 0C5, Canada

[c] State Key Laboratory of Metastable Materials Science and Technology, Yanshan University, Qinhuangdao 066004, China

[d] Department of Environmental Science and Engineering, Keimyung University, Daegu 42601, Republic of South Korea

[#] Contribution equal

[*] Corresponding Authors

E-mail address: liuchao198967@126.com (Chao Liu), gousechem@gmail.com (Shaik Gouse Peera) and liang_tx@126.com (Tongxiang Liang).

Table S1 Formation energy (E_f) and Binding energies (E_b) in eV for various types of Ni-N-C-gra configurations.

	NiN_4	NiN_3C	NiN_2C_2-p	NiN_2C_2-h	NiN_2C_2-o	$NiNC_3$
E_f	-4.20	-3.29	-2.05	-2.41	-1.86	-0.58
E_b	7.21	8.04	9.50	8.32	8.94	8.46
	NiC_4	NiN_3	NiN_2C	$NiNC_2$	NiC_3	
E_f	1.07	-1.42	-0.66	-0.06	0.60	
E_b	6.84	4.73	5.49	5.61	7.11	

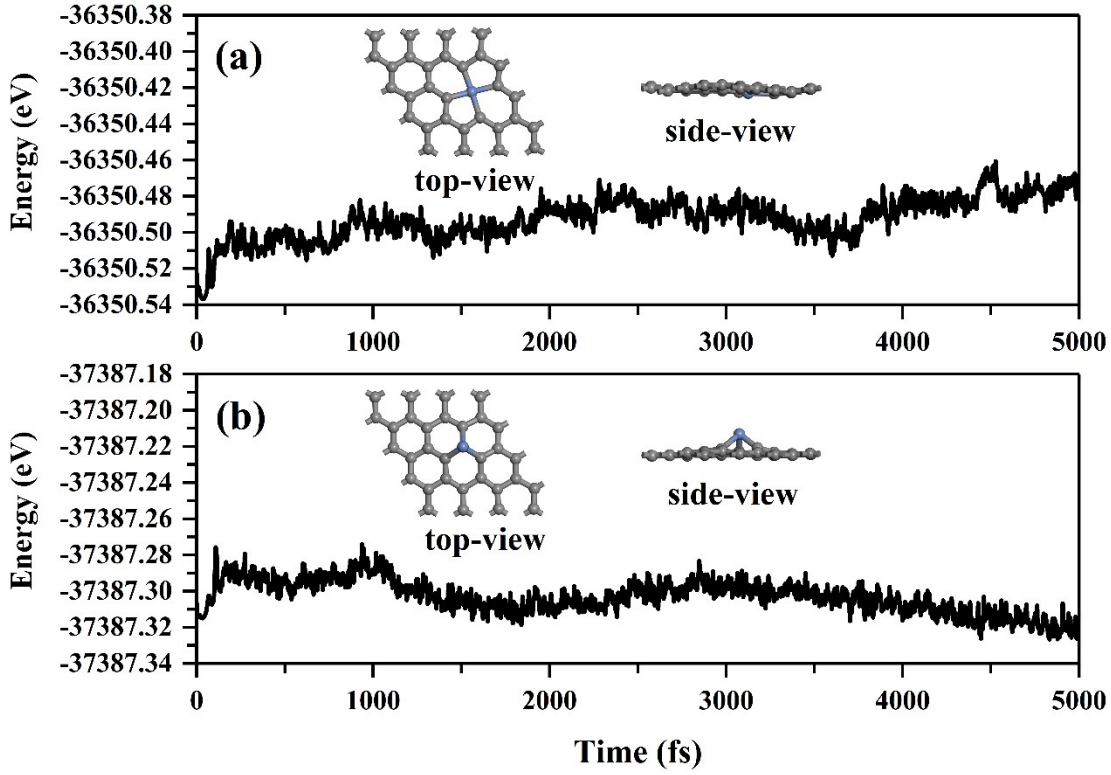

Fig. S1 Total energy change of (a) NiC_4 and (b) NiC_3 at 5 ps during MD simulations at 500 K, as well as top and side snapshots of the structures at the end of 5 ps.

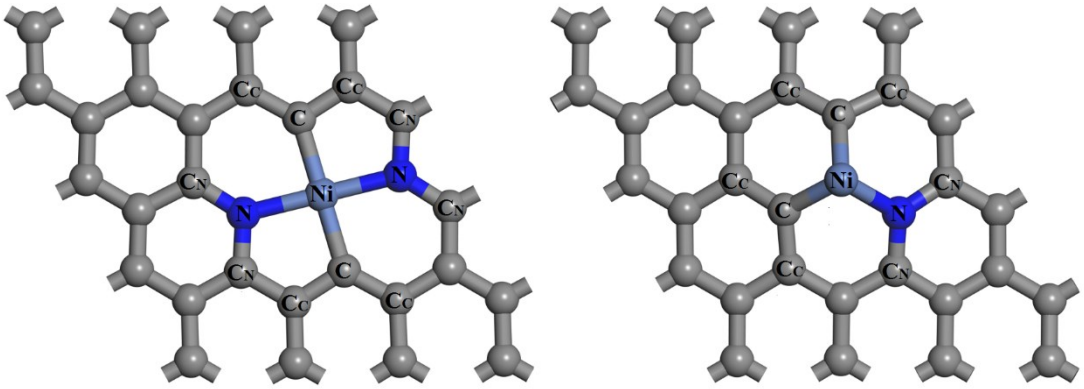

Fig. S2 Classify atoms according to element type and relative position.

Table S2 Q(Ni), Q(N) and Q(C) refer to the charge on Ni atom, N and C atoms adjacent to Ni atom, respectively. $Q(C_N)$ and $Q(C_C)$ represent the charge of the outer C atoms of N, C atoms connected to Ni atom, as shown in Fig. S2. The positive and negative numbers represent electrons lost and gained, respectively, based on the analysis of Mulliken charge (Q in e).

	Q(Ni)	**Q(N)**	**Q(C)**	**$Q(C_N)$**	**$Q(C_C)$**
NiN_4	0.135	-1.672		1.644	
NiN_3C	0.004	-1.269	-0.012	1.279	-0.012
NiN_2C_2-p	-0.110	-0.814	-0.108	0.810	0.138
NiN_2C_2-h	-0.116	-0.868	-0.012	0.946	-0.057
NiN_2C_2-o	-0.067	-0.824	-0.134	0.908	0
$NiNC_3$	-0.116	-0.417	-0.204	0.458	0.110
NiC_4	-0.187		-0.330		0.252
NiN_3	0.446	-1.328		1.188	
NiN_2C	0.278	-0.918	-0.070	0.814	0.023
$NiNC_2$	0.149	-0.484	-0.130	0.411	0.094
NiC_3	0.039		-0.266		0.164

Table S3 The adsorption configurations of $*O_2$, *OOH, *O and *OH on various types of Ni-N-C-gra (including hydroxylated Ni-N-C-gra).

	$*O_2$		*OOH	*O	*OH
	side-on	end-on			
NiN_4		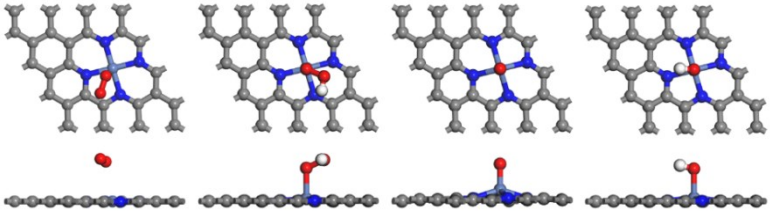			
NiN_3C		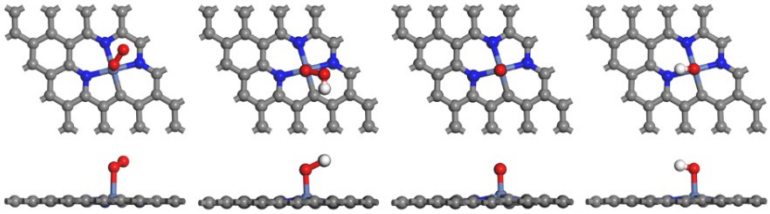			
NiN_2C_2-p		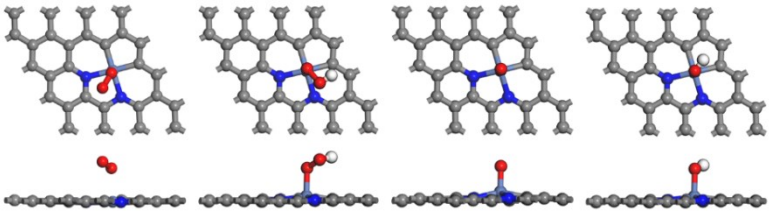			
NiN_2C_2-h		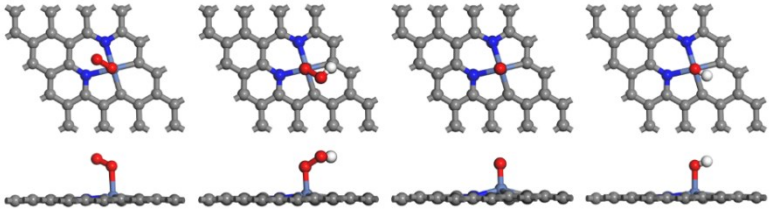			
NiN_2C_2-o	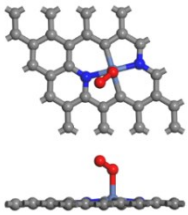	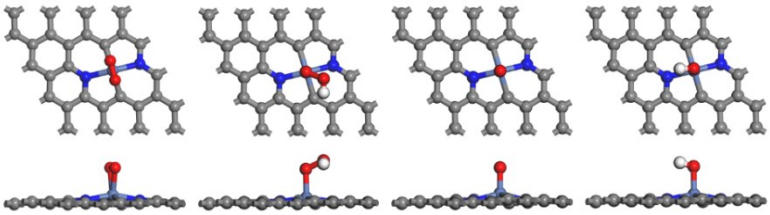			
$NiNC_3$	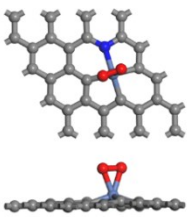	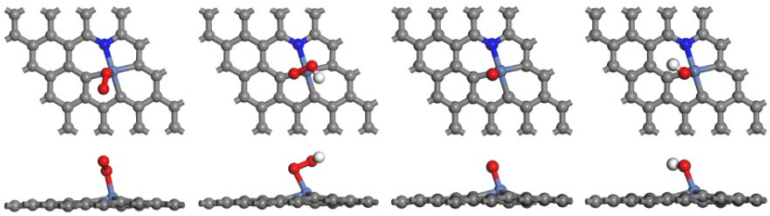			

NiC_4	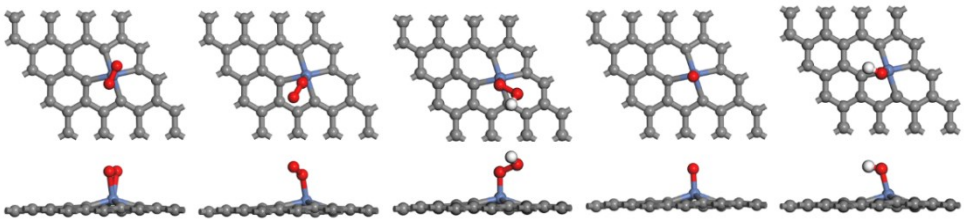
NiN_3	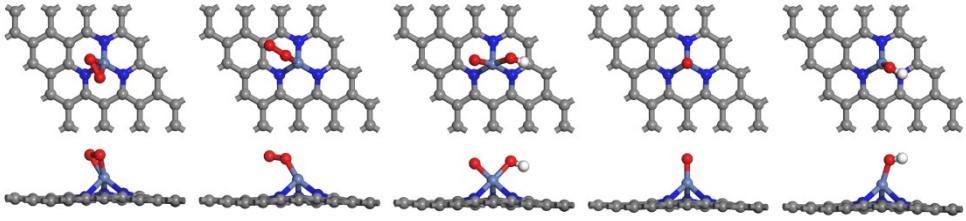
NiN_2C	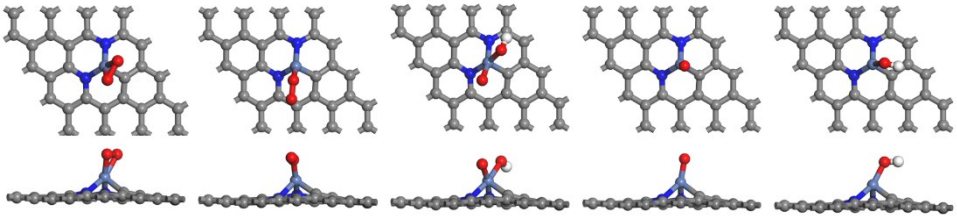
$NiNC_2$	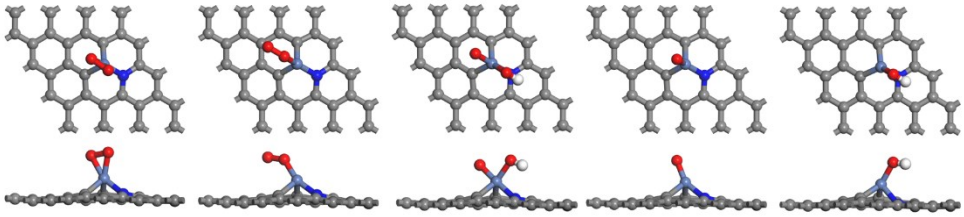
NiC_3	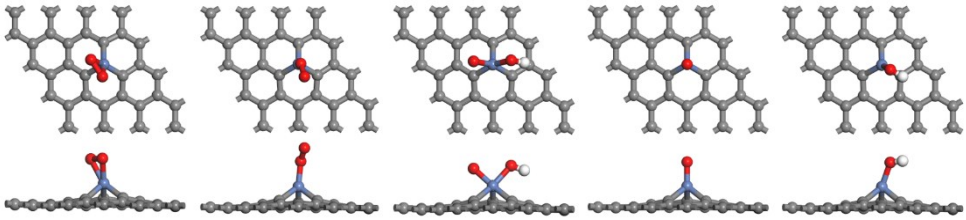
$Ni(OH)N_3$	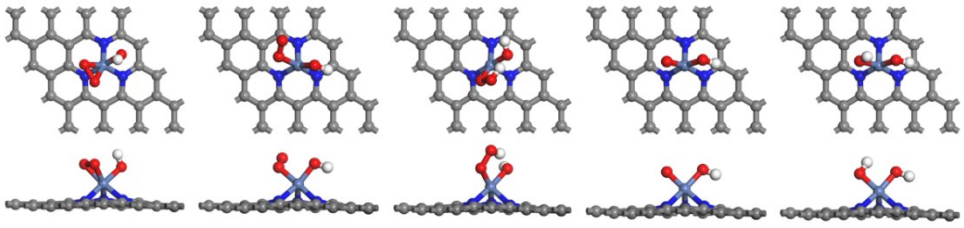
$Ni(OH)N_2C$	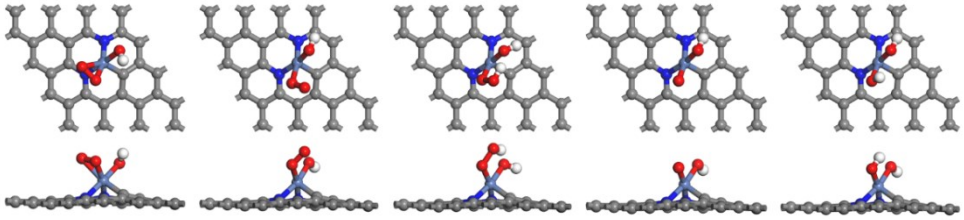

$Ni(OH)NC_2$	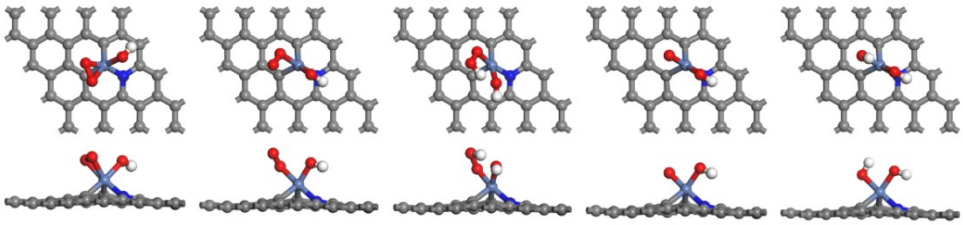				
$Ni(OH)C_3$	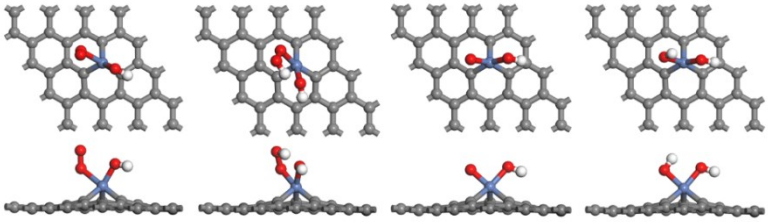				

[a](blank) No stable adsorption configuration was obtained in geometric optimization.

Table S4 Adsorption energy data (ΔE_{ads}, eV) of reactive species on Ni-N-C-gra (including hydroxylated Ni-N-C-gra).

	$\Delta E_{*O_2(side\text{-}on)}$	$\Delta E_{*O_2(end\text{-}on)}$	ΔE_{*OOH}	ΔE_{*O}	ΔE_{*OH}
NiN_4		-0.29	-0.60	-2.05	-1.61
NiN_3C		-0.36	-0.83	-2.25	-1.90
NiN_2C_2-p		-0.30	-0.86	-2.43	-1.94
NiN_2C_2-h		-0.36	-0.85	-2.49	-1.94
NiN_2C_2-o	-0.12	-0.38	-0.84	-2.54	-1.91
$NiNC_3$	-0.51	-0.42	-1.06	-2.84	-2.17
NiC_4	-0.72	-0.64	-1.38	-3.30	-2.52
NiN_3	-2.51	-1.90	-3.34	-5.00	-4.00
NiN_2C	-2.24	-1.87	-3.22	-4.94	-3.83
$NiNC_2$	-2.08	-1.60	-2.88	-4.92	-3.72
NiC_3	-1.84	-1.29	-2.55	-5.08	-3.76
$Ni(OH)N_3$	-0.87	-0.86	-1.87	-3.19	-2.85
$Ni(OH)N_2C$	-0.91	-0.86	-1.87	-3.25	-2.92

$Ni(OH)NC_2$	-0.52	-0.71	-1.72	-3.02	-2.74
$Ni(OH)C_3$		-0.46	-1.53	-2.65	-2.48

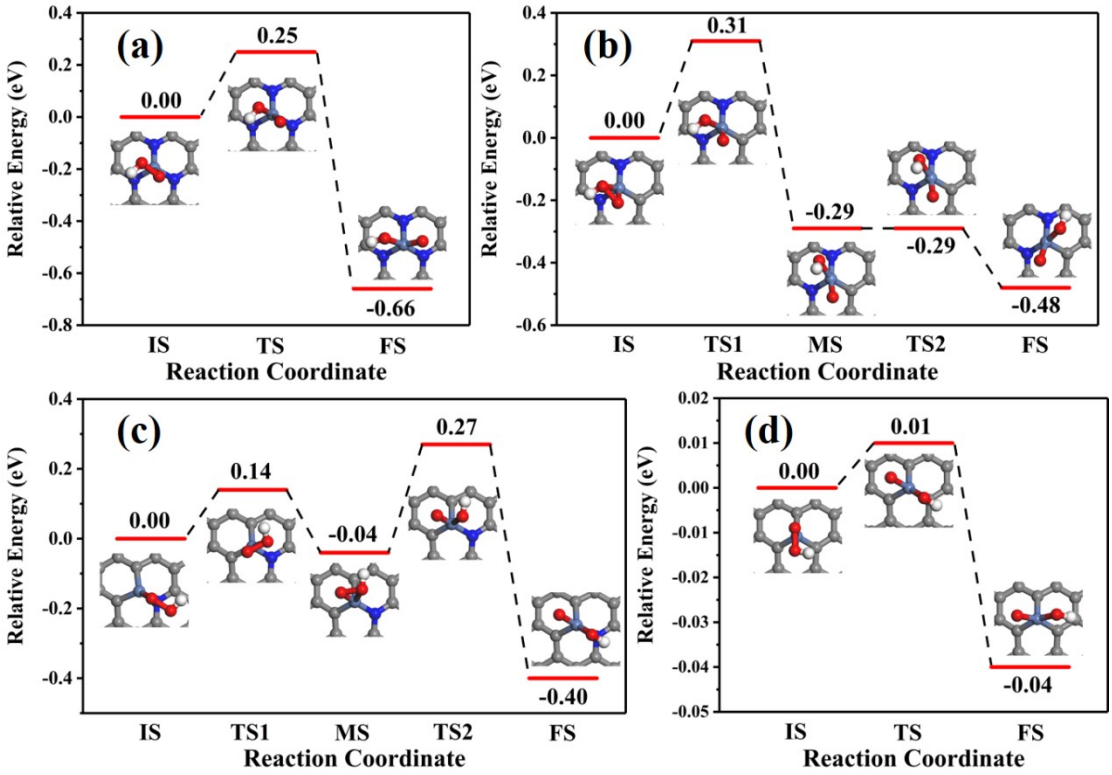

Fig. S3 Optimized structures of the initial state (IS), transition state (TS), mediate state (MS), and final state (FS) of OOH dissociation on three-coordination catalysts and corresponding energy barriers for the reaction:

Table S5 Free energy changes of ΔGx (x=1-4, eV) and overpotential (η, V) of ORR/OER on four-coordination Ni-N-C-gra.

		ΔG1	**ΔG2**	**ΔG3**	**ΔG4**	**η**
NiN_4	**ORR**	0.77	-0.28	-1.09	-1.00	1.17
	OER	1.00	1.09	0.28	-0.77	0.69
NiN_3C	**ORR**	0.59	-0.25	-1.20	-0.75	1.00
	OER	0.75	1.20	0.25	-0.59	0.80

NiN_2C_2-p	**ORR**	0.58	-0.41	-1.05	-0.73	0.98
	OER	0.73	1.05	0.41	-0.58	0.65
NiN_2C_2-h	**ORR**	0.57	-0.44	-1.04	-0.69	0.97
	OER	0.69	1.04	0.44	-0.57	0.64
NiN_2C_2-o	**ORR**	0.59	-0.52	-0.95	-0.73	0.99
	OER	0.73	0.95	0.52	-0.59	0.55
$NiNC_3$	**ORR**	0.43	-0.68	-0.83	-0.52	0.83
	OER	0.52	0.83	0.68	-0.43	0.43
NiC_4	**ORR**	0.08	-0.80	-0.70	-0.18	0.48
	OER	0.18	0.70	0.80	-0.08	0.40

Table S6 Free energy changes (ΔG, eV) and overpotential (η, V) of ORR on three-coordination Ni-N-C-gra.

Pathway 1	$\Delta G_{O_2 \rightarrow (*O + *OH)}$	$\Delta G_{(*O + *OH) \rightarrow *O}$	$\Delta G_{*O \rightarrow *OH}$	$\Delta G_{*OH \rightarrow OH^-}$	**η**
NiN_3	-1.86	-0.44	-0.63	1.33	1.73
NiN_2C	-1.73	-0.60	-0.45	1.17	1.57
$NiNC_2$	-1.43	-0.82	-0.36	1.00	1.40
NiC_3	-1.04	-1.30	-0.32	1.06	1.46
Pathway 2	$\Delta G_{O_2 \rightarrow (*O + *OH)}$	$\Delta G_{(*O + *OH) \rightarrow 2*O}$	$\Delta G_{2*OH \rightarrow *OH}$	$\Delta G_{*OH \rightarrow OH^-}$	**η**
NiN_3	-1.86	-1.12	0.05	1.33	1.73
NiN_2C	-1.73	-1.17	0.12	1.17	1.57
$NiNC_2$	-1.43	-1.20	0.03	1.00	1.40
NiC_3	-1.04	-1.31	-0.31	1.06	1.46

Table S7 Free energy changes (ΔG, eV) and overpotential (η, V) of OER on three-coordination Ni-N-C-gra.

Pathway 1	$\Delta G_{OH^- \rightarrow *OH}$	$\Delta G_{*OH \rightarrow *O}$	$\Delta G_{*O \rightarrow (*O + *OH)}$	$\Delta G_{(*O + *OH) \rightarrow (*OOH +}$	$\Delta G_{(*OOH + *OH) \rightarrow *}$	**η**
NiN_3	-1.33	0.63	0.44	0.24	0.30	0.23
NiN_2C	-1.17	0.45	0.60	0.26	0.30	0.20
$NiNC_2$	-1.00	0.36	0.82	0.20	0.23	0.42
NiC_3	-1.06	0.32	1.30	-0.02	0.01	0.90
Pathway 2	$\Delta G_{OH^- \rightarrow *OH}$	$\Delta G_{*OH \rightarrow 2*OH}$	$\Delta G_{2*OH \rightarrow (*O + *OI}$	$\Delta G_{(*O + *OH) \rightarrow (*OOH +}$	$\Delta G_{(*OOH + *OH) \rightarrow *}$	**η**
NiN_3	-1.33	-0.05	1.12	0.24	0.30	0.72
NiN_2C	-1.17	-0.12	1.17	0.26	0.30	0.77
$NiNC_2$	-1.00	-0.03	1.20	0.20	0.23	0.80
NiC_3	-1.06	0.31	1.31	-0.02	0.01	0.91

Fig. S4 Various adsorption configurations of H_2O_2 on three-coordination catalysts.

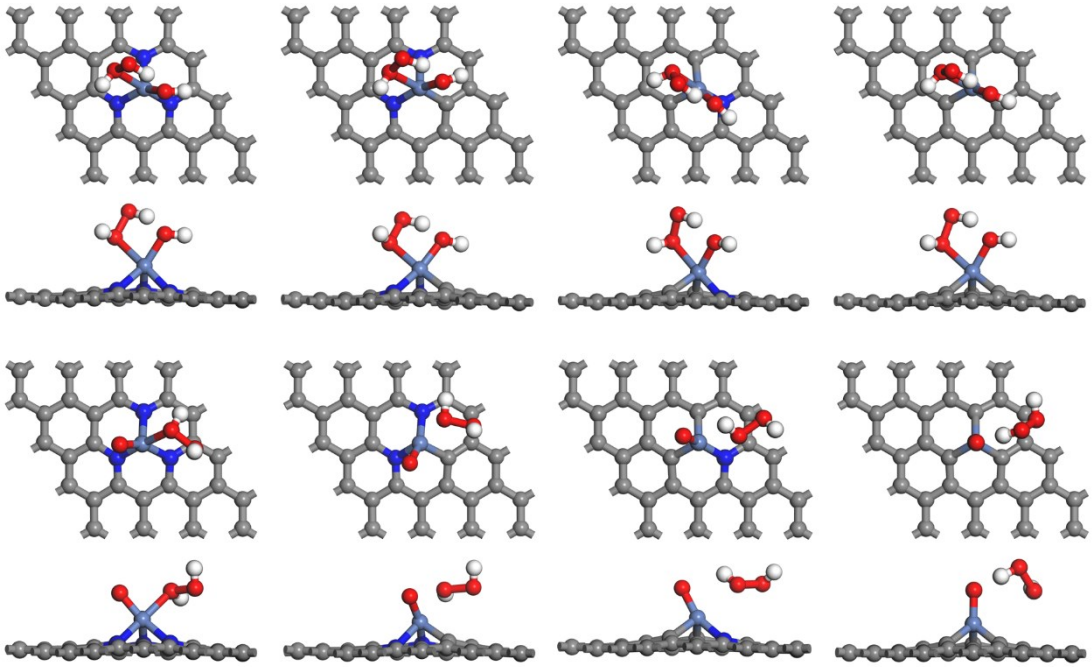

Table S8 Free energy change (ΔG, eV) of H_2O_2 formation.

	$\Delta G_{(*O+*OH)\rightarrow(*O+H_2O_2)}$	$\Delta G_{2*OH\rightarrow(*OH+*H_2O_2)}$
NiN_3	1.68	1.99
NiN_2C	1.52	1.86
$NiNC_2$	1.30	1.99
NiC_3	0.82	1.58

Table S9 Free energy changes of ΔG_X (x=1-4) and overpotential (η) of ORR on hydroxylated Ni-N-C-gra.

		ΔG1	ΔG2	ΔG3	ΔG4	η
$Ni(OH)N_3$	**ORR**	-0.30	-0.24	-1.12	0.05	0.45
$Ni(OH)N_2C$	**ORR**	-0.30	-0.26	-1.17	0.12	0.52

$Ni(OH)NC_2$	**ORR**	-0.23	-0.20	-1.20	0.03	0.43
$Ni(OH)C_3$	**ORR**	0	0.02	-1.31	-0.31	0.42

Table S10 Adsorption free energies (ΔG_{ads}, eV) of the intermediate species (*OOH, *O and *OH) adsorbed on various Ni-N-C-gra configurations (including Ni-N-C-gra).

	ΔG_{*OOH}	ΔG_{*O}	ΔG_{*OH}		ΔG_{*OOH}	ΔG_{*O}	ΔG_{*OH}
NiN_4	4.86	3.75	1.83	**NiN_3**	2.23	0.97	-0.50
NiN_3C	4.68	3.61	1.58	**NiN_2C**	2.36	0.93	-0.34
NiN_2C_2-p	4.67	3.43	1.56	**$NiNC_2$**	2.66	1.01	-0.17
NiN_2C_2-h	4.66	3.39	1.52	**NiC_3**	3.05	0.92	-0.23
NiN_2C_2-o	4.68	3.34	1.56	**$Ni(OH)N_3$**	3.79	2.73	0.78
$NiNC_3$	4.52	3.01	1.35	**$Ni(OH)N_2C$**	3.79	2.70	0.71
NiC_4	4.17	2.54	1.01	**$Ni(OH)NC_2$**	3.86	2.83	0.80
				$Ni(OH)C_3$	4.09	3.28	1.14

Table S11 Mulliken charge population on Ni, N, C, C_N and C_C atoms of each Ni-N-C-gra with an adsorbed O_2. The positive and negative values in the brackets represent the loss and accumulation of electrons after $*O_2$ adsorption, respectively. (Q in e)

	Q($*O_2$)	Q(Ni)	Q(N)	Q(C)	Q(C_N)	Q(C_C)
NiN_4	-0.196	0.156	-1.640		1.694	
		(0.021)	(0.032)		(0.050)	
NiN_3C	-0.266	0.083	-1.236	-0.002	1.309	0.006
		(0.079)	(0.033)	(0.010)	(0.030)	(0.018)
NiN_2C_2-p	-0.189	-0.046	-0.800	-0.095	0.822	0.129
		(0.064)	(0.014)	(0.013)	(0.012)	(-0.009)
NiN_2C_2-h	-0.229	-0.019	-0.851	-0.011	0.957	-0.020
		(0.097)	(0.017)	(0.001)	(0.011)	(0.037)
NiN_2C_2-o	-0.235	0.030	-0.828	-0.111	0.924	0.036
		(0.097)	(-0.004)	(0.023)	(0.016)	(0.036)
$NiNC_3$	-0.324	0.005	-0.410	-0.144	0.461	0.148
		(0.121)	(0.007)	(0.060)	(0.003)	(0.038)
NiC_4	-0.266	-0.059		-0.266		0.273
		(0.128)		(0.064)		(0.021)
NiN_3	-0.611	0.421	-1.240		1.362	
		(-0.025)	(0.088)		(0.174)	
NiN_2C	-0.612	0.298	-0.876	0.038	0.923	0.099
		(0.020)	(0.042)	(0.108)	(0.109)	(0.076)
$NiNC_2$	-0.605	0.181	-0.439	-0.046	0.455	0.166
		(0.032)	(0.045)	(0.084)	(0.044)	(0.072)
NiC_3	-0.577	0.058		-0.104		0.205
		(0.019)		(0.162)		(0.041)

Table S12 Mulliken charge population on Ni, N, C, C_N, C_C and *OH of each hydroxylated Ni-N-C-gra. The positive and negative values in the brackets represent the loss and accumulation of electrons, respectively. (Q in e)

	Q(Ni)	Q(N)	Q(C)	Q(C_N)	Q(C_C)	Q(*OH)
Ni(OH)N_3	0.463	-1.293	0	1.283		-0.413
Ni(OH)N_2C	0.312	-0.921	0.034	0.854	0.057	-0.331
Ni(OH)NC_2	0.141	-0.433	-0.078	0.365	0.120	-0.363
Ni(OH)C_3	0.069	0	-0.170		0.186	-0.343

Table S13 Mulliken charge population on Ni, N, C, C_N, C_C and *OH of each hydroxylated Ni-N-C-gra with an adsorbed O_2. The positive and negative values in the brackets represent the loss and accumulation of electrons after *O_2 adsorption, respectively. (Q in e)

	Q(*O_2)	Q(Ni)	Q(N)	Q(C)	Q(C_N)	Q(C_C)	Q(*OH)
Ni(OH)N_3	-0.517	0.366	-1.160	0	1.458		-0.288
		(-0.097)	(0.133)		(0.175)		(0.125)
Ni(OH)N_2C	-0.392	0.230	-0.823	0.027	0.929	0.099	-0.271
		(-0.082)	(0.098)	(-0.007)	(0.075)	(0.042)	(0.060)
Ni(OH)NC_2	-0.274	0.152	-0.432	-0.059	0.418	0.171	-0.323
		(0.011)	(0.001)	(0.019)	(0.053)	(0.051)	(0.040)
Ni(OH)C_3	-0.256	0.028	0	-0.123		0.212	-0.308
		(-0.041)		(0.047)		(0.026)	(0.035)

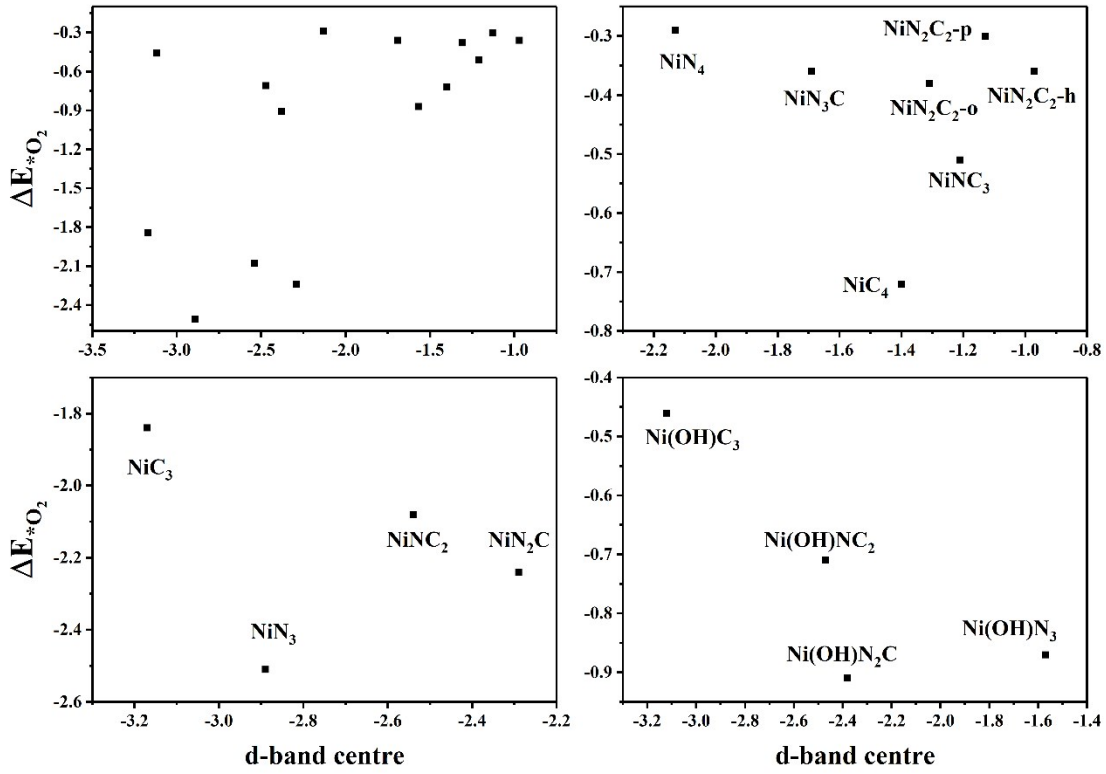

Fig. S5 The relationship between oxygen adsorption energy and d-band center. (Integral range -∞ to +∞, $\varepsilon_d = \frac{\int_{-\infty}^{+\infty} \rho(\varepsilon)\varepsilon d\varepsilon}{\int_{-\infty}^{+\infty} \rho(\varepsilon) d\epsilon}$, where ρ are the densities of states and ε are the energies.)

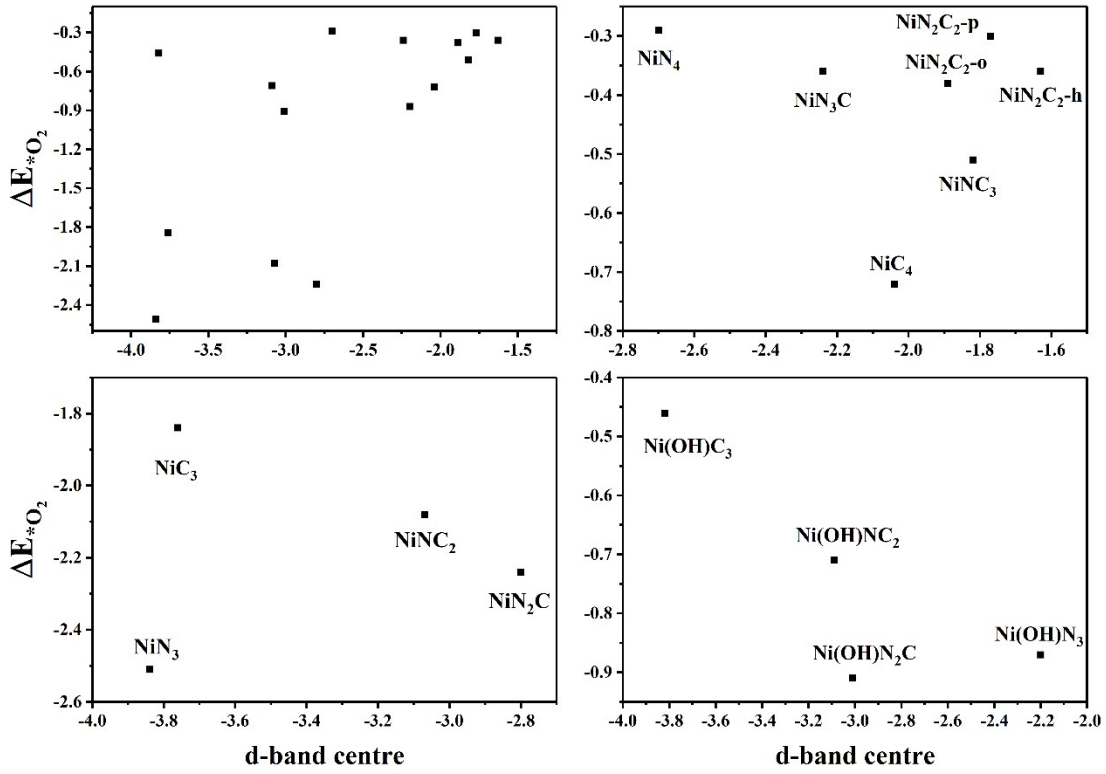

Fig. S6 The relationship between oxygen adsorption energy and d-band center. (Integral range -∞ to E_F(Fermi level), $\varepsilon_d = \frac{\int_{-\infty}^{E_F} \rho(\varepsilon)\varepsilon d\varepsilon}{\int_{-\infty}^{E_F} \rho(\varepsilon) d\epsilon}$, where ρ are the densities of states and ε are the energies.)

Table S14 Values of PDOS abundance near Fermi level (D_F) in different intervals.

$D_F = \int_{-x}^{x} \rho(\varepsilon) d\varepsilon$	(-0.2, 0.2)	(-0.5, 0.5)	(-0.7, 0.7)	(-1, 1)
NiN_4	0.02	0.09	0.22	1.09
NiN_3C	0.10	0.34	0.94	2.40
NiN_2C_2-p	0.72	2.13	3.15	4.42

NiN_2C_2-h	1.23	2.97	3.88	5.39
NiN_2C_2-o	0.35	1.37	2.44	3.85
$NiNC_3$	0.43	1.41	2.56	4.25
NiC_4	0.49	0.97	1.35	2.63
NiN_3	0.29	1.42	1.59	1.91
NiN_2C	0.29	0.83	1.20	1.88
$NiNC_2$	0.13	0.65	1.11	1.61
NiC_3	0.09	0.54	1.00	1.33
$Ni(OH)N_3$	0.59	1.38	2.06	3.26
$Ni(OH)N_2C$	0.14	0.63	1.14	1.89
$Ni(OH)NC_2$	0.25	0.86	1.16	1.42
$Ni(OH)C_3$	0.18	0.29	0.41	0.91